Signatures of nonadiabatic O_2 dissociation at Al(111): First-principles fewest-switches study

Christian Carbogno,[1] Jörg Behler,[2] Karsten Reuter,[3] and Axel Groß[1]

[1]*Institut für Theoretische Chemie, Universität Ulm, D-89069 Ulm, Germany*
[2]*Lehrstuhl für Theoretische Chemie, Ruhr-Universität Bochum, D-44780 Bochum, Germany*
[3]*Fritz-Haber-Institut der Max-Planck-Gesellschaft, Faradayweg 4-6, D-14195 Berlin, Germany*

(Dated: September 30, 2009)

Recently, spin selection rules have been invoked to explain the discrepancy between measured and calculated adsorption probabilities of molecular oxygen reacting with Al(111). In this work, we inspect the impact of nonadiabatic spin transitions on the dynamics of this system from first principles. For this purpose the motion on two distinct potential-energy surfaces associated to different spin configurations and possible transitions between them are inspected by means of the Fewest Switches algorithm. Within this framework we especially inspect the influence of such spin transitions on observables accessible to molecular beam experiments. On this basis we suggest experimental setups that can validate the occurrence of such transitions and discuss their feasibility.

PACS numbers: 31.50.Gh, 68.35.Ja, 68.43.Bc, 82.20.Gk

I. INTRODUCTION

Metal oxidation processes are of outstanding importance in various industrial fields which range from combustion catalysis to microelectronics. Accordingly, this research field has attracted huge scientific interest—both from experimentalists and theorists—over the last decades. Although the most fundamental rules underlying such processes were understood[1] quite early, there still exist some not yet elucidated phenomena, even for systems that appear utterly simple at first sight. One of the most prominent and intriguing examples is the oxidation of the (111) surface of aluminum which exhibits various astonishing features. The exposure of a clean aluminum surface to an oxygen atmosphere leads to the growth of an oxide film, which then inhibits further corrosion. In spite of the fact that the overall mechanism for the formation of this Al_2O_3 stoichiometry has already been elucidated by qualitative[2] kinetic considerations, the elementary key steps underlying this process are still topic of a lively scientific debate.

For instance, scanning tunneling microscopy (STM) images obtained after exposing the clean aluminum surface to a minute dosage of molecular oxygen show only single oxygen atoms in an average distance of more than 80 Å from each other[3] on the surface. Various hypotheses, e.g., the subsurface migration of single oxygen atoms[4] or a cannonball like abstraction dynamics[5–7] of the impinging oxygen molecules, have been proposed to explain this extraordinary finding. As a matter of fact, even the validity of the original experiment has been questioned[8]. The contradictory nature of the proposed mechanisms, which are all backed up by reasonable scientific findings, already shows how complicated the experimental clarification of this issue is.

However, at first sight the questions should be settled easily by means of the current available simulation techniques[9]. Unfortunately, this is not the case for this particular system: Various studies carried out on the basis of state-of-the-art adiabatic density functional theory (DFT)[10,11] were not even able to qualitatively reproduce the low adsorption probability for thermal O_2 molecules at the clean aluminum surface found[12] in molecular beam experiments. If even the simulation of such an elementary key step of the reaction fails that dramatically, attempts to model the more complex features of the dissociation dynamics within the framework provided by DFT are foredoomed to fail, too.

Recently, however, DFT calculations addressing potential energy surfaces (PESs) of fixed spin states were able to reproduce the experimental data in a semiquantitative way. These studies suggest that spin selection rules, which hinder[13] an adiabatic spin transition from the initial O_2 gas-phase triplet state to the singlet state of the adsorbed O atoms, are the rate determining factor in this process. For these investigations a constrained density functional theory approach[14] was employed to compute the PESs of O_2 in different spin-configurations, and the lowered adsorption probability was then correctly reproduced when restricting[15] the O_2 molecules to move on the spin-triplet potential-energy surface only.

Although these studies yield a more than qualitative correspondence with the experiment with respect to the initial sticking coefficient, they inherently incorporate an approximation that is not satisfactory ultimately. By restricting the motion to the triplet PES alone, the impinging O_2 molecules are not able to relax to the correct final singlet state of the adsorbed atoms while dissociating. Therefore we extend these previous studies by considering the dissociation dynamics on multiple spin potential-energy surfaces, allowing transitions between them within the mixed quantum-classical *Fewest Switches*[16] algorithm as proposed by Tully, which has been successfully employed in the modeling of various[17,18] molecule-surface processes before. As detailed below, we can thereby reproduce the measured sticking coefficient and thus reconfirm the earlier more restricted

modeling. Additionally, our simulations allow to study the occurrence, the nature and the influence of the spin transitions in detail. On the basis of these calculations, we were already able to propose[19] measurements that can clearly prove the nonadiabaticity of the studied reaction. In this work we further study such potential experimental setups and especially focus on their feasibility. Therefore, we explicitly inspect how various uncertainties underlying the theoretical modeling, as for instance the frozen substrate approximation, affect the practical realization of such scattering experiments in the lab.

The proposed measurements can verify the fundamental assumption behind our approach that hindered spin transitions are indeed the rate determining factor in this process. This is of particular importance due to the fact that speculations[20,21] have arisen which do not relate the low sticking coefficient of thermal oxygen molecules to the nonadiabatic dynamics. Rather, shortcomings of the state-of-the-art but still approximative exchange-correlation GGA functional employed in the DFT calculations are held responsible for the discrepancy found between the adiabatic simulations and the experiment. Such conjectures are hard to confute theoretically, at least as long as calculations with an improved exchange-correlation functional are numerical too costly to be performed accurately on a large scale. Certainly, this dictates also further research along these lines. However, the herein proposed experiments can clarify this severe doubt already now and thus establish a solid founding for further research on the complex phenomena associated with the oxidation of aluminum surfaces.

In this paper we will first review the *ab initio* methods underlying the simulations in Sec. II. Since the DFT techniques used for the calculation of the total energy of the system as well as the techniques employed to interpolate this set of data to a smooth potential-energy surface have already been discussed in detail[14,22] before, we will focus on the method used to calculate the dynamics on multiple potential-energy surfaces, i.e., Tully's Fewest Switches[16] algorithm. Especially, we will discuss the nature of the simulated electronic states and the nonadiabatic coupling between them. In Sec. III we will then present the result of such simulations, whereby a special focus lies on the occurrence and on the role of the nonadiabatic transitions. In this context we will also present possible experimental approaches able to identify the occurrence of the spin transitions, whereby we will also discuss the feasibility of the proposed experiments. We especially focus on the uncertainties underlying the employed theoretical approach and try to quantify them by additionally inspecting the influence of different coupling strengths and the role of the surface mobility.

II. THEORETICAL METHODS

A. Mixed Quantum-Classical Dynamics

When inspecting the dynamics of a system that includes nonadiabatic transitions, the electronic and nuclear degrees of freedom cannot be tackled independently and subsequently, as done in the Born-Oppenheimer approximation. Unfortunately, a full quantum dynamical description of both the electronic and nuclear degrees of freedom is computationally far too demanding for the present system. However, for the nuclei usually a classical treatment is sufficient. Still, the fast electronic and slow nuclear degrees of freedom have to be inspected simultaneously, whereby a mutual self-consistent feedback between them is crucial[23] to achieve a correct description of the system. In this work we employ a mixed quantum-classical method, namely the *Fewest Switches Surface Hopping* algorithm as proposed by Tully[16], to achieve this goal. For a concise summary of this approach, the total Hamiltonian for a system including electronic ($\mathbf{r}$) and nuclear ($\mathbf{R}$) degrees of freedom

$$\begin{aligned} H &= T_{\mathbf{R}} + T_{\mathbf{r}} + V_{\mathbf{r}} + V_{\mathbf{rR}} + V_{\mathbf{R}} \\ &= T_{\mathbf{R}} + H_{el}(\mathbf{r},\mathbf{R}) + V_{\mathbf{R}} \end{aligned} \tag{1}$$

will serve as a starting point. In Eq. (1), T denotes the kinetic energy operators, V the respective electrostatic potentials and all terms depending on the electronic coordinates are subsumed in H_{el}. The total wave function for this system can then be expressed as

$$\Psi(\mathbf{r},\mathbf{R},t) = \sum_i c_i(t)\Phi_i(\mathbf{r},\mathbf{R}) \ , \tag{2}$$

whereby the basis functions $\Phi_i(\mathbf{r},\mathbf{R})$ used in the expansion, also referred to as electronic states in this work, are not necessarily eigenfunctions of the electronic Hamiltonian H_{el}. For each of these basis functions, we can derive a Hamilton-Jacobi equation for the nuclear dynamics, in which the potential

$$V_{ii}(\mathbf{R}) = \langle \Phi_i(\mathbf{r},\mathbf{R}) | \, H_{el}(\mathbf{r},\mathbf{R}) + V_{\mathbf{R}} \, | \Phi_i(\mathbf{r},\mathbf{R}) \rangle \tag{3}$$

resulting from the integration over the electronic degrees of freedom indicated by the bra-ket notation, is specific to the thereby employed basis function $\Phi_i(\mathbf{r},\mathbf{R})$. Consequently, an equation of motion for each particular electronic state included in the expansion (2) can be derived. Whenever the nuclear masses of interest are significantly larger than the one of hydrogen, so that quantum effects in the dynamics of the slow degrees of freedom can be safely neglected[24], the motion can be described by classical equations of motion

$$M\frac{d^2}{dt^2}\mathbf{R} = -\nabla_{\mathbf{R}} V_{ii}(\mathbf{R}). \tag{4}$$

Still, these equations do just describe the motion on one single PES but not the transitions between different PESs.

If we insert the full expansion (2) into the time-dependent Schrödinger equation associated with the Hamiltonian H, we gain a set of coupled differential equations[16,17]

$$i\hbar\dot{c}_k = \sum_j c_j(t)\left(V_{kj}(\mathbf{R}(t)) - i\hbar\dot{\mathbf{R}}(t)\cdot\mathbf{d}_{ij}(\mathbf{R}(t))\right), \quad (5)$$

which describe how the expansion coefficients related to the individual electronic states evolve along a trajectory $\mathbf{R}(t)$. Beside the non-diagonal potential matrix elements $V_{kj}(\mathbf{R}(t))$, also the *nonadiabatic coupling vector*

$$\mathbf{d}_{ij}(\mathbf{R}) = \langle\Phi_i(\mathbf{r},\mathbf{R})|\,\nabla_{\mathbf{R}}\,|\Phi_j(\mathbf{r},\mathbf{R})\rangle\,, \quad (6)$$

which designates the dependence of the chosen basis functions $\Phi_i(\mathbf{r},\mathbf{R})$ on the nuclear positions, enters the equations. By integrating Eq. (5) along a trajectory, the changes in the occupation of the different electronic states during the dynamics, i.e., the time evolution of the diagonal elements of the density matrix $a_{ij}(t) = c_i(t)^* c_j(t)$, can be inspected for a specific trajectory.

This fact can be exploited to combine Eq. (4) and (5) to a surface hopping method: At each time step Δt, the system is in exactly **one** electronic state k that determines which potential V_{kk} is used in Eq. (4) to compute the classical trajectory. On the other hand, the complete set of equations (5) is integrated along the trajectory to determine the occupation in **all** electronic states of the expansion. If by any chance another electronic state from the one that actually determines the nuclear dynamics becomes dominant, the trajectory "switches" to this state: From then, this new state will determine the potential in the nuclear equation of motion, as long as no other switch occurs. To actually decide whether and when such a "surface hop" occurs, a Metropolis[25] like algorithm is combined with the switching probability proposed by Tully[16]

$$P_{k\to j}(t) = \frac{\dot{a}_{jj}(t)}{a_{kk}}\Delta t\,. \quad (7)$$

This so called *Fewest Switches* approach, which distinguishes this method from comparable surface hopping approaches (see Ref. [23] and references therein), fulfills two essential conditions. For a large number of computed trajectories, the population in each state statistically matches the probabilities given by the density matrix a_{ii}. Thereby, this distribution is achieved with as few surface hops as possible. Please note that this algorithm allows switches to occur at any point along the trajectory $\mathbf{R}(t)$, even if the potential energies differ (e.g., $\Delta V = V_{jj}(\mathbf{R}) - V_{kk}(\mathbf{R}) \neq 0$). For such surface hops with $\Delta V \neq 0$, special care has to be taken with respect to energy conservation. If the kinetic energy of the nuclei is smaller than the potential difference ($T_{\mathbf{R}} < \Delta V$), the switches are rejected. Conversely, if the potential energy difference is larger than the kinetic energy ($T_{\mathbf{R}} > \Delta V$), the velocities have to be rescaled to fulfill $T^j_{\mathbf{R}} - T^k_{\mathbf{R}} = -\Delta V$. This constraint is not unique because the direction of the velocity adjustment can be chosen freely. Considerations from semi-classical theory suggest to rescale the velocities along the nonadiabatic coupling vector, since the forces associated with nonadiabatic transitions typically[26,27] point in its direction.

Although the herein given description of the Fewest Switches method is adequate to understand the calculations presented below, it is certainly not exhausting. The interested reader is referred to the original publications describing this method[16,23,28].

B. The inspected electronic states

The first essential step in the simulation of nonadiabatic reactions with the surface hopping method is the identification of the electronic states of interest, i.e., the basis used for the expansion (2). Since a distinct PES $V_{ii}(\mathbf{R})$, which has usually to be calculated individually under huge numerical effort, is associated to each one of these electronic states, it is desirable to achieve a correct description of the system with as few expansion terms as possible. Fortunately, the inclusion of the adiabatic ground state and one additional excited state is typically already sufficient to model nonadiabatic processes accurately[23]. In our case an analysis of the adiabatic calculation—a so called *diabatization*—serves as a starting point for the determination of the electronic states that are relevant in the inspected system's dynamics, since such a *diabatic*[62] representation allows for a more natural and intuitive interpretation of the occurring electronic transitions.

As shown for an exemplary geometry in Fig. 1, the PES associated with the initial state of the reaction, i.e., the triplet ground state of the isolated oxygen molecule, resembles the adiabatic ground state PES closely at large molecule-surface distances and is thus the first state included in the surface hopping approach. Not too surprisingly, this triplet PES does not coincide with the adiabatic PES in the limit of small oxygen-surface distances: In this final state of the reaction, the dissociated oxygen atoms adsorbed on the surface exhibit a singlet type ground state electronic structure, whereby an additional charge transfer[10,14] from the surface onto the molecule occurs. Although there might be multiple charged states of the oxygen molecule involved[29] in the actual electron transfer process, we can qualitatively incorporate such effects in this schematic model by one effective PES. This so called ionic PES resembles the adiabatic potential closely in the late part of the dynamics and approaches the lowest lying charge-transfer state in the vacuum limit. Its respective energy gap can be estimated from the clean aluminum surfaces work function and the isolated oxygen molecules electron affinity to be 4 eV with respect to the triplet ground state. In between these two states, two additional singlet states of the neutral oxygen molecule, i.e., the $^1\Delta_g$ and the $^1\Sigma_g^+$ state, are located. Although these two states do neither correspond

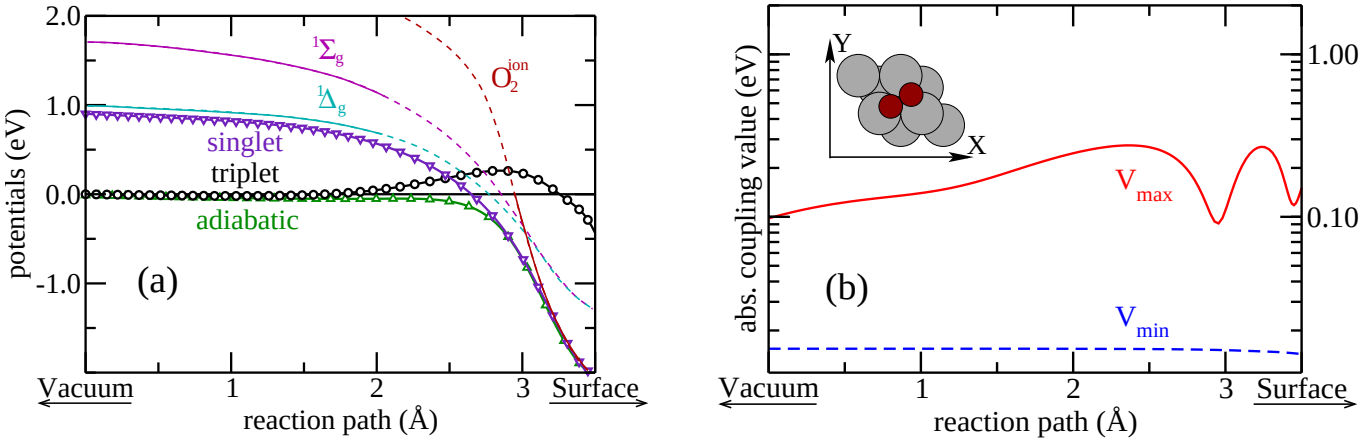

FIG. 1: Schematic plot of the potential-energy surfaces along the minimum energy path in the triplet state for dissociation in parallel alignment over the fcc site: Beside the adiabatic (spin-polarized), the triplet (constrained spin-polarized) and the singlet (adiabatic non-spin-polarized) PESs, which have been determined by means of DFT, also the expected functional form of the potentials associated with the first two excited singlet states and the so-called "ionic" state are shown in Fig. (*a*). In Fig. (*b*) the lower and the upper bound derived for the coupling of the triplet and the singlet PES are plotted along the minimum energy path of Fig. (*a*).

to the initial nor to the final state of the reaction, they play a crucial role in the dynamics. In the proximity of the barriers present on the triplet PES they definitely are as relevant as the respective triplet and ionic PES, since they exhibit comparable curve crossings with the triplet state.

It would certainly be desirable to include all of these excited states in the simulation of the nonadiabatic dynamics. However, even the first principles calculation of one single PES alone is utterly costly in terms of computing power. But even more importantly, the $^1\Delta_g$ and the $^1\Sigma_g^+$ state exhibit a strongly correlated, multi-determinant wave function[14,15,30] that is not described correctly by single-determinant theories such as Hartree-Fock and DFT. As a matter of fact, the current exchange-correlation functionals, which do not depend on the symmetry of the electronic structure, do not allow to discriminate[31,32] between the $^1\Delta_g$ and the $^1\Sigma_g^+$ state at all. This becomes evident already when inspecting the **isolated** oxygen molecule by an adiabatic non-spin-polarized DFT calculation, which must yield a singlet state by construction. In this approach, however, the respective wave functions of the two singlet states mix[33] in equal parts, so that the resulting triplet-singlet gap lies between the correct values that are associated with the $^1\Delta_g$ and the $^1\Sigma_g^+$ state respectively. When additionally including the aluminum slab in such an adiabatic non-spin-polarized DFT calculation, the actual triplet-singlet gap is lowered due to a spurious and unphysical charge transfer from the surface that occurs even at large molecule-surface separations: The current GGA exchange-correlation functionals erroneously favor such a charge separation due to their incorrect convexity with respect to fractional charges[34]. As a consequence the thereby computed PES mimics the first excited $^1\Delta_g$ singlet state at large distances from the surface, as shown in Fig. 1. In proximity of the surface, this PES coincides with the one associated with the adiabatic ground state, since the charge transfer between oxygen and aluminum is not restrained in the underlying adiabatic non-spin-polarized DFT calculations. Thus such an approach enables us to effectively describe both the charge transfer effects close to the surface as well as the influence of the neutral singlet states within **one** single PES. However, such an approximative but still adequate description of the manifold of excited states also has some drawbacks. For the calculation of the coupling elements we have to disentangle the contributions from the various electronic states once again, as discussed in the next section.

For the sake of readability the adiabatic spin-polarized PES will henceforth be referred to as "adiabatic", the constrained spin-polarized triplet PES as "triplet" and the adiabatic non-spin-polarized PES as "singlet". All three potential energy surfaces, which explicitly depend on the six degrees of freedom of the oxygen molecule, have been constructed in the frozen substrate approximation by interpolating large sets of *ab initio* data. A detailed discussion of the underlying constrained and unconstrained DFT simulations[14,15], of the neural network interpolation[22] and of the dynamics on a single PES[13,15] can be found in the cited publications.

C. The Coupling

For the derivation of the coupling elements we will again rely on the diabatic representation (see Sec. II B) of the triplet and the singlet state ($|\Psi_t\rangle, |\Psi_s\rangle$), for which the nonadiabatic coupling vector

$$\mathbf{d}_{ts}(\mathbf{R}) = \langle\Psi_t| \nabla_{\mathbf{R}} |\Psi_s\rangle = 0 \tag{8}$$

vanishes exactly at each point in space due to the trivially fulfilled orthogonality of the respective spinors. Consequently, the evolution of the density matrix in Eq. (5)—and hence the electronic transitions—is completely determined by the non-diagonal elements of the electronic Hamiltonian

$$V_{ts} = \langle \Psi_t | \, \mathcal{H}_e \, | \Psi_s \rangle \, . \tag{9}$$

To disentangle the various interactions contributing to this coupling, we decompose the singlet wave function, which is actually a mixture of three distinct states (see Sec. II B), into its individual components:

$$\Psi_s = A \cdot \left(\frac{1}{\sqrt{2}} \left(\Psi_\Delta + \Psi_\Sigma \right) \right) + B \cdot \Psi_{\text{ion}}, \tag{10}$$

i.e., the first excited $^1\Delta_g$ singlet state Ψ_Δ, the second excited $^1\Sigma_g^+$ singlet state Ψ_Σ and the "ionic" state Ψ_{ion}, which adiabatically incorporates all charge transfer effects and is identical to the singlet ground state close to the surface. Thereby the complex parameters A and B are determined by the adiabatic mixing of the neutral and the ionic state described before.

In a first step, we neglect the contributions arising from the coupling to the ionic state and focus on the isolated molecule in the vacuum limit, where no charge transfer is supposed to happen. Under these assumptions the coupling can be simplified to:

$$V_{ts} = \frac{1}{\sqrt{2}} \left(\langle \Psi_t | \, \mathcal{H}_e \, | \Psi_\Delta \rangle + \langle \Psi_t | \, \mathcal{H}_e \, | \Psi_\Sigma \rangle \right) . \tag{11}$$

Since the spinors present on the left and on the right hand side of the Hamiltonians in Eq. (11) are orthogonal to each other, the only interaction that does not vanish in the evaluation of this matrix element is the spin-orbit coupling (SOC)

$$V_{ts} = \frac{1}{\sqrt{2}} \left(\langle \Psi_t | \, V_{\text{SOC}} \, | \Psi_\Delta \rangle + \langle \Psi_t | \, V_{\text{SOC}} \, | \Psi_\Sigma \rangle \right) . \tag{12}$$

The first of the two coupling terms in Eq. (12), i.e., the SO coupling of the triplet ground state to the first excited $^1\Delta_g$ singlet state, vanishes in first order approximation, since selection rules prohibit a direct mixing of the two states[35,36]. Solely, an indirect coupling[37,38] through the highly excited $^3\Pi_g$ state, which is at least two orders of magnitude smaller than the direct SO coupling of the triplet ground state to the $^1\Sigma_g^+$ state discussed below, is possible. Thus the overwhelming portion of the spin-orbit coupling is provided by the second term, i.e., the SO coupling of the triplet ground state to the second excited $^1\Sigma_g^+$ singlet state. For the isolated oxygen molecule, this non-diagonal matrix element has been calculated as a function of the oxygen-oxygen distance with the SOC module[39] provided by the quantum chemical simulation package *Molpro*[40] on the basis of wave functions determined[63] by *Multireference Configuration Interaction*[41] before. The thereby determined coupling V_{ts}—as well as the derived lifetime of 11.16 s for the $^1\Sigma_g^+$ state—is in excellent agreement with experimental and theoretical data found in literature[35,36,42]. With respect to the oxygen-oxygen separation, which is the only degree of freedom the coupling actually depends on in these calculations, it is a linear, slowly decreasing (almost constant) function, even up to huge separations (see Fig. 1). If even a factual dissociation of the isolated molecule does not affect this coupling, also the interaction with the aluminum, which exhibits only a small SOC[43] due to its low mass, will not alter it significantly. Consequently,

$$V_{\min} = \frac{1}{\sqrt{2}} \langle \Psi_t | \, V_{\text{SOC}} \, | \Psi_\Sigma \rangle \, , \tag{13}$$

the absolute value of which is plotted in Fig. 1, can be regarded as a lower boundary for the true coupling present in the system.

On the basis of this minimal coupling determined above and the PESs described in Sec. II B we can construct the diabatic potential matrix

$$\mathbb{H} = \begin{pmatrix} \langle \Psi_t | \, \mathcal{H}_e \, | \Psi_t \rangle & \langle \Psi_t | \, \mathcal{H}_e \, | \Psi_s \rangle \\ \langle \Psi_s | \, \mathcal{H}_e \, | \Psi_t \rangle & \langle \Psi_s | \, \mathcal{H}_e \, | \Psi_s \rangle \end{pmatrix} = \begin{pmatrix} E_t & V_{\min} \\ V_{\min}^* & E_s \end{pmatrix} \tag{14}$$

and diagonalize it to obtain the respective adiabatic representation of the potentials

$$E_{\text{adia}} = \frac{1}{2} \left(E_s + E_t \pm \sqrt{\left(E_s - E_t \right)^2 + 4 \left| V_{\min} \right|} \right) \tag{15}$$

for this minimal coupling. Due to its minute value, however, only a small deviation from the diabatic potentials occurs at all, as already evident from the minute gap of approximately $2V_{\min} \approx 30$ meV at the avoided crossing point. This fact also highlights the main shortcoming of this minimal coupling element: The minute splitting at the avoided crossing is not able to recover the adiabatic ground state potential that has been determined by the unconstrained DFT calculations before. However, this fact also allows to turn the tide: By forcing the left hand side of Eq. (15) to correspond to the adiabatic potential determined by DFT before, we can invert the diagonalization to obtain a complementary value for the coupling element

$$|V_{\max}| = \sqrt{E_s E_t - E_s E_{\text{adia}}^{\text{DFT}} - E_t E_{\text{adia}}^{\text{DFT}} + \left(E_{\text{adia}}^{\text{DFT}} \right)^2} . \tag{16}$$

In contrast to the one-dimensional minimal coupling, this coupling term $|V_{\max}|$ is a true six-dimensional function of the oxygen coordinates, since the inverse diagonalization (16) can be evaluated at each point in space for which respective triplet, singlet and adiabatic potential values are available. Accordingly, this coupling also depends on the respective rotational and center of mass degrees of freedom so that it does not exhibit such a constant behavior along the minimum energy path as the SOC (see Fig. 1). Due to the spurious charge transfer occurring

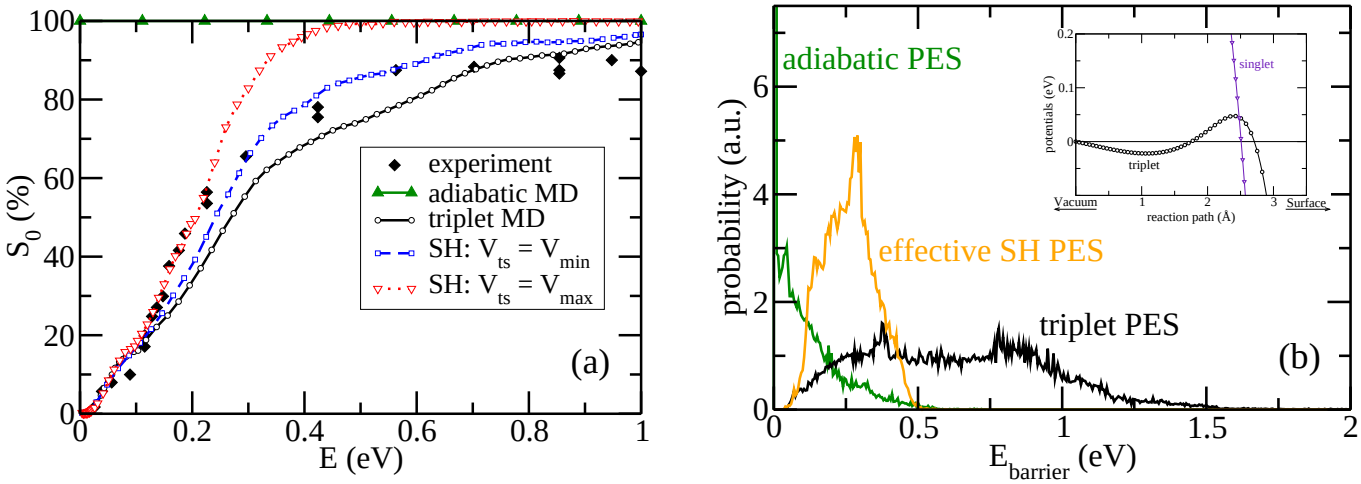

FIG. 2: (*a*) Sticking coefficient $S_0(E)$ as computed by molecular dynamics (MD) on the triplet potential-energy surface and by Tully's surface hopping method (SH) for both a maximal and a minimal coupling of the triplet and the singlet PES. The respective experimental data[12] is shown as well. (*b*) Area-normalized histograms of the barriers found on the individual PESs by the two-dimensional Nudged Elastic Band technique (see text). The potentials along the minimum energy path over the bridge site are shown in the inset.

in the adiabatic calculations, however, this maximal coupling does not vanish in the vacuum limit as one would expect. Additionally, the inverse diagonalization procedure itself is generally expected to overestimate the coupling[44], so that $V_{\max}$ can be regarded as an upper bound for the true coupling present in the system. In fact we believe that the maximal coupling is closer to the true coupling strength than the minimal coupling.

In the case of such a maximal coupling, a diagonalization of the respective diabatic Hamiltonian matrix yields a ground state potential that resembles the adiabatic PES exactly, as required by construction. Consequently all barriers previously present in the diabatic picture vanish as well, so that surface hopping simulations of thermal molecules, for which the diabatic calculations yield a sticking probability of 2% (see Sec. III A), lead to a constant sticking coefficient of 100% in the adiabatic picture. This alarming discrepancy between the two representations can be traced back to our approximative description of the manifold of excited states by a single effective PES. In the limit of a large coupling our model describes the two-level system consisting of the triplet and the ionic state, but does not account for the presence of the other two neutral singlet states.

In the diabatic picture this is indeed a justified approximation, since due to the minute coupling the two singlet states just provide for a negligible amount of additional nonadiabatic transitions with respect to the ionic state. This is no longer true in the adiabatic picture: In this representation, the potential-energy surfaces of states that are strongly coupled are also strongly distorted at avoided curve crossings. The smaller the coupling of the respective states is in the diabatic picture, however, the more probable transitions between the adiabatic PES become. By not including the singlet states and their minute coupling in the adiabatic representation of our two-level model, we are de facto ignoring the adiabatic PES that matters most, i.e., the one to which a transition will almost certainly occur at the avoided crossing. To avoid these problems without the cumbersome construction of another PES (see Sec. II B), we performed all the calculations presented here in the diabatic representation. The price to pay is that the effective barriers in the simulations are slightly overestimated, since nuclear tunneling effects and resonances, which would be inherently incorporated[23] in an adiabatic picture, are neglected in such a diabatic representation. Fortunately, these effects are typically negligible in high-dimensional, heavy systems[45,46] such as the one addressed in this work.

D. Calculational Details

In all presented MD and SH simulations the initial conditions are chosen to model a molecule in the vacuum limit, in which it does not interact with the aluminum surface. Therefore the initial center-of-mass distance between the oxygen and the surface is always 5 Å. Also, a certain amount of energy E is assigned to the translational motion perpendicular to the surface. The initial oxygen-oxygen distance and vibration is chosen to model the zero point energy of the free molecule ($\approx$ 0.1 eV) in the so called quasiclassical approximation[24]. In the beginning no kinetic energy is assigned to the rotational and to the lateral center-of-mass degrees of freedom, but their initial values are also chosen randomly to uniformly examine all possible initial conditions. To sample the whole phase space and to converge the calculations with respect to the electronic transitions at least 2,000 trajectories have been computed for each of the data points

in the following figures. When a higher accuracy was needed, as in Sec. III B for instance, up to $2,000,000$ trajectories have been computed. In each case the calculation of the individual trajectories is stopped when one of the following conditions is reached: Molecules are regarded as dissociated, if the oxygen-oxygen distance exceeds 2.0 Å ($\approx 160\%$ of the equilibrium bond length of the free molecule), and as reflected, if the center-of-mass distance to the surface exceeds 5 Å. The maximal time interval for one trajectory is chosen so that virtually all molecules eventually fulfill one of these two conditions.

Naturally, the convergence of the results with respect to the presented calculational details and with respect to the numerical integration routines has been examined extensively[50].

III. RESULTS AND DISCUSSION

A. The Sticking Coefficient

The sticking coefficient $S_0(E)$ at normal incidence, i.e., the probability of dissociative adsorption as a function of the incident translational energy E for a molecular beam oriented perpendicular to the surface, is the basic observable that we are going to discuss while investigating the nonadiabatic dynamics of this system. As shown in Fig. 2, it exhibits an S-like shape in the experiments—a typical evidence for an activated process. MD calculations on the adiabatic PES alone, however, yield a sticking coefficient of constantly 100% even at thermal incident energies[13] due the almost complete absence of barriers[14,47] on the respective PES. Conversely, MD simulations on the triplet PES reproduce the measurements more than satisfactorily, as already discussed in the introduction.

With respect to the MD simulations performed on the triplet PES alone[13,15], the inclusion of nonadiabatic transitions within the surface hopping method changes the simulated sticking coefficient only quantitatively, but not qualitatively. At large incidence energies there is obviously no substantial difference at all: The impinging oxygen is able to overcome the barriers anyway, regardless of any occurring electronic transitions. In contrast to this, molecules at medium velocities are not always able to overcome the barriers on the triplet PES. Whereas such molecules are repelled in the triplet MD calculations, they can dissociate by switching to the singlet PES in the SH simulations, as soon as they reach the respective crossing point (see Fig. 1a). The probability for such an electronic transition to occur depends on the coupling of the two electronic states so that the relative increase in dissociation found in the SH simulations varies with the coupling strength. Last but not least, the triplet MD and the SH simulations yield the same sticking coefficient at the smallest incident energies below 150 meV: Molecules that are not even capable of reaching the crossing point are also not able to benefit from the possibility of an electronic transition. This might seem surprising at first, since one might expect at least some triplet-singlet crossing points to occur also in this low energy regime. However, this is not the case: As exemplarily shown for the bridge site in the inset of Fig. 2b, the crossing point and the top of the barrier almost coincide even in geometries that exhibit barriers well below 150 meV. As a consequence, the sticking coefficient is not affected by the switches in these setups, in spite of the fact that there is a high probability for such transitions at these low velocities.

These effects can be studied more systematically on the basis of the actual barrier heights that the molecules experience on the individual PESs in the sudden approximation. To determine this statistical distribution we inspected the minimum energy path on a large number of elbow plots by a two-dimensional, self-implemented[64] *Climbing-Image Nudged Elastic Band*[48,49] method. Both the histograms of the barriers found on the adiabatic PES and on the triplet PES are shown in Fig. 2b. The effective barriers experienced by the impinging molecules in the surface hopping simulations, however, depend on the probability for an electronic transition and thus both on the coupling and on the velocity of the molecules. At fast velocities and for a minute coupling, the molecules stay on the triplet PES and thus behave as in the triplet MD simulations. In this limit, the barrier distribution of the triplet state describes the dynamics best. Conversely, the impinging molecules switch to the singlet state almost instantaneously while bypassing the crossing seam at low velocities and for huge couplings. In this limit, the energetic location of the crossing points can be regarded as an *effective barrier* distribution.

As shown in Fig. 2b, the average height of these effective barriers has also been determined[65] by means of the *Climbing Image Nudged Elastic Band* method. The resulting barrier distributions substantiate the previous findings of the simulations: The adiabatic PES is unactivated for the large majority of geometries and even in the case of a hindered dissociation the arising barriers are typically smaller than 0.5 eV. In contrast to this, the triplet PES exhibits exclusively activated entrance channels with a broad distribution of barriers that ranges from approximately 40 meV up to more than 1.5 eV. These barriers are drastically reduced by the occurrence of electronic transitions at the crossing points, the energetic height of which is 0.5 eV at most. However, the lowest occurring barriers are not modified due to the reasons discussed before.

Please note that the great majority of these barriers lies in the entrance channel, i.e., before the oxygen molecule starts to dissociate and the oxygen atoms move apart. Accordingly, no distinct influence of the vibrational state on the dissociation probability is expected. Nevertheless, the slight vibrational enhancement found in the experiment[12] at small incident energies can be reproduced[50] by the simulations and can be traced back to an effective lowering of the barriers due to an adiabatic

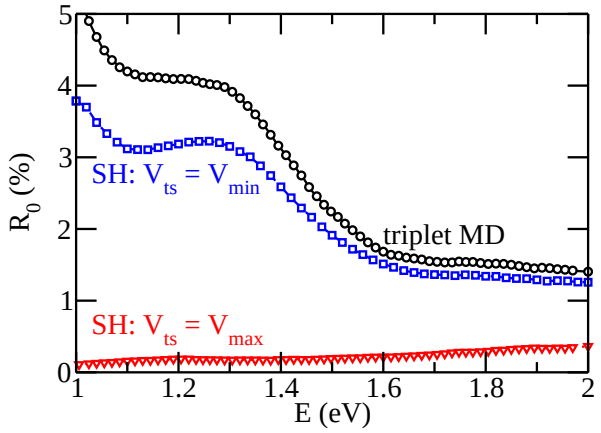

FIG. 3: Reflection coefficient at high incident translational energies as computed by MD on the triplet PES and by Tully's surface hopping method (SH) for a minimal and a maximal coupling of the triplet and the singlet PES.

energy transfer[51] occurring in the nuclear dynamics from the vibrational degree of freedom onto the translational one.

B. High Energy Scattering

Although the hitherto presented simulations reproduce the experimental data successfully, this does not explicitly prove the hypothesis[13] that nonadiabatic spin-transitions indeed play a decisive role in the dynamics of the triplet oxygen molecules at the aluminum surface. Therefore we searched for a possible experimental setup that is able to unambiguously demonstrate the occurrence of such transitions. The fact that the triplet PES exhibits barriers as high as 1.5 eV might indeed offer a route towards experimental verification: For incident energies that are larger than the triplet-singlet gap ($\approx$ 1 eV), energy conservation does no longer prohibit a conversion of triplet into singlet molecules during the backscattering. If such singlet molecules were detected in the reflection channel, the nonadiabaticity of the scattering process could be experimentally proved.

To investigate the feasibility of such a measurement, we focus on the reflection coefficient $R_0(E) = 1 - S_0(E)$, i.e., the probability for a molecule with perpendicular incidence to be repelled back into the vacuum as a function of the initial translational energy E. As shown in Fig. 3, we indeed find a small amount of molecules ($< 5\%$) that are reflected in the triplet MD simulations due to the barriers on the triplet PES. The larger the incident energies, the less probable such backscattering events obviously become. For incident energies above 1.5 eV, for which the triplet PES does not exhibit any barriers anymore, the reflection coefficient does however not drop to zero but levels off at a value of 1.4 %. In this energy regime, the translational movement is so fast that the oxygen

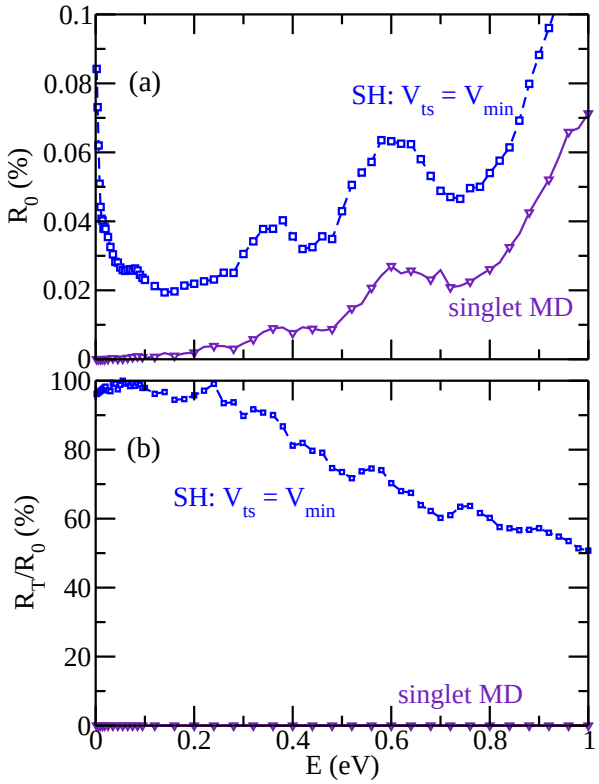

FIG. 4: (a) Reflection coefficient R_0 as function of the incident kinetic energy of singlet oxygen molecules, as calculated by the SH method with a minimal coupling. Additionally, the respective data obtained by MD simulations on the singlet PES alone is shown. (b) Relative triplet yield R_T/R_0 for both calculations.

molecules approaching the surface in an unfavorable geometry are not able to dissociate in the small time interval before being backscattered, since they do not follow the minimum energy path anymore.

Not too surprisingly, the SH simulations with a minimal coupling closely resemble the triplet MD calculations. For such huge velocities and a minute coupling, oxygen behaves diabatically, i.e., it just stays on the triplet PES in almost all trajectories. In contrast to this, in the simulations with maximal coupling a significant amount of molecules still relaxes to the singlet PES, which exhibits no barriers, as soon as the crossing point is passed. Accordingly, the associated SH simulations yield only a minute reflection coefficient that slightly **increases** with larger incident energy. Even for such a huge coupling, the probability for electronic transitions decreases with larger velocities, so that for large incident energies more and more molecules stay on the more repulsive triplet PES and are backscattered. Still, this effect is almost negligible, even for the fastest molecules. Regardless of the coupling, the already small reflection probabilities are even further diminished as soon as one gives up the frozen substrate approximation (see Sec. III D). Even worse, less than 3% of these reflected molecules are

found in the singlet state upon reflection, so that only 0.01% of all incident molecules result in a backscattered singlet molecule at most, even in in the frozen substrate approximation. This fact makes an experimental detection of the nonadiabatic transition in the presented way factually impossible.

C. Singlet Scattering

The sticking coefficient $S_0(E)$ of triplet molecules discussed above does not provide an unambiguous experimental evidence for the occurrence of nonadiabatic spin-transitions. This is principally caused by the fact that this typically inspected observable is not particularly sensitive to the occurring electronic transitions. For the same reason also a pure triplet MD approach yields a more than satisfactory agreement with the experimental data (see Sec. III A). To actually nail down the influence of the spin-transitions on the reaction dynamics experimentally, a complementary process that is significantly more sensitive to the transitions has to be found. Indeed, we could identify[19] the dissociative adsorption of singlet oxygen molecules to provide for experimental observables that strongly depend on the occurrence of such spin-transitions. A comparable strategy has already been used in a recent combined experimental and theoretical study[52] to demonstrate the importance of spin selection rules for O_2 interacting with small Al anion clusters (∼10 to 20 atoms). In this work, an odd/even pattern in the reactivity of triplet oxygen has been found as a function of the number n of atoms in the Al clusters, whereas no such pattern has been found for the reaction of singlet molecules with these clusters. These studies motivated further studies addressing the dynamics of singlet oxygen, for example in the combination with other metal surfaces such as Ag(100)[53].

In our simulations we studied the dynamics of singlet oxygen molecules impinging in normal incidence on the aluminum surface at various kinetic energies. In the following, we will concentrate on two complementary observables that will allow us to understand the nonadiabatic processes active in the reaction. Firstly, we will inspect the **total** amount of backscattered molecules as function of the incident translational energy, i.e., the *reflection coefficient* $R_0(E)$. In a second step, we will also inspect the **relative** amount of molecules that are backscattered in the triplet state, i.e, the *relative triplet yield* $R_T(E)/R_0(E)$, which turns out as the actual fingerprint of the nonadiabatic transition.

As shown in Fig. 4, the probability of backscattering rises with increasing kinetic energy in the case of a minimal coupling: Although the singlet PES does not exhibit any barriers at all, some molecules at high velocities are reflected on this PES before the oxygen molecules are able to dissociate. The higher the incident energy, the more probable such a process obviously becomes. Therefore the respective SH simulations resemble MD simulations on the singlet PES closely, apart from a constant offset. This difference is caused by the fact that in the backscattering process a reallocation of the translational energy onto the other degrees of freedom occurs. Such vibrational or rotational excited molecules might not have the translational energy to escape the surface on the singlet PES anymore. While such molecules are trapped in the surface's proximity and then finally dissociate in the singlet MD calculations, such molecules can escape in the SH simulations by switching to the triplet PES thus gaining the energy of the singlet-triplet splitting which helps them to leave the surface. This mechanism leads to an exponentially increasing reflection coefficient at small incident energies, for which almost all backscattered molecules leave the surface in the triplet state.

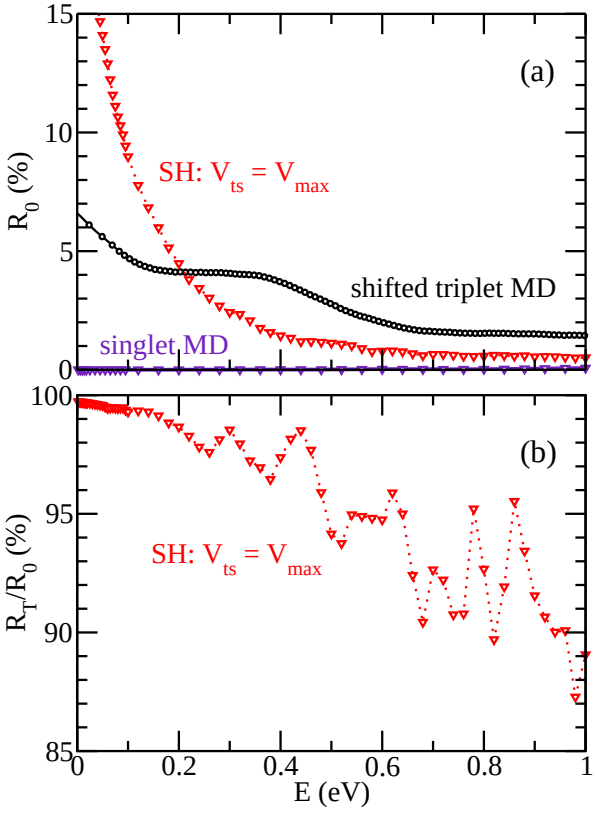

FIG. 5: Same as Fig. 4, but for maximal coupling.

Intuitively one might expect the same mechanism to be active also in the case of the maximal coupling (see Fig. 5). This is indeed the case at large incident energies, for which a small amount of molecules is backscattered on the singlet PES and then partially escapes the surface in the triplet state. The increased coupling favors the transition to the triplet state and thus increases both the total amount of reflected molecules as well as the relative fraction of triplet oxygen. A totally different mechanism, which is not active in the simulations with the minimal coupling, causes an exponential increase of the reflection coefficient for low and medium incident energies in the simulations with the maximal coupling. When approach-

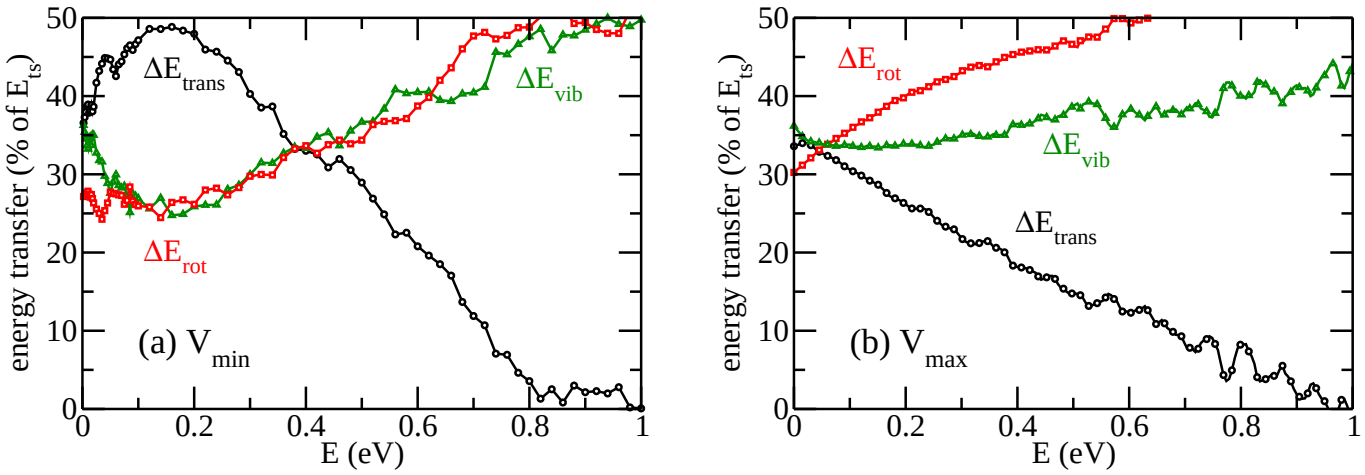

FIG. 6: Average kinetic energy gained by singlet molecules when being converted to triplet molecules in the backscattering process at the aluminum surface for a (*a*) minimal coupling; (*b*) maximal coupling.

ing the surface, the strong coupling destabilizes the singlet state, so that a decay to the triplet ground state becomes extremely probable even while the crossing seam is approached. Thus the great majority of the molecules hit the surface on the triplet PES, on which there are barriers as high as 1.5 eV present (see Fig. 2b), so that a backscattering event is orders of magnitude more likely than on the unactivated singlet PES. Consequently, one would expect the singlet's reflection probability to be similar to the one of triplet molecules that hit the surface with a comparable kinetic energy $E + \Delta E_{\rm ts}$.

A comparison with such a shifted triplet MD reflection coefficient surprisingly reveals that the respective reflection probability of the singlet molecules is even higher, as shown in Fig. 5. During the nonadiabatic relaxation to the triplet state, which does not exclusively occur at the crossing point but also in its proximity where the two PESs do not coincide, the surplus of potential energy is reallocated onto all degrees of freedom. Since this allotment is performed along the nonadiabatic coupling vector (see Sec. II), not all the potential energy stored in the triplet-singlet gap $E_{\rm ts}$ is transferred onto the translational degrees of freedom, which are principally responsible for surmounting the barriers. Rather, also the vibrational, rotational and lateral center-of-mass degrees of freedom, which do not promote the dissociation as strongly or might even hinder it, gain a certain portion of kinetic energy, which is then missing in the perpendicular translational motion. Consequently, these simulations are not directly comparable to the triplet MD, in which the complete amount $E + \Delta E_{\rm ts}$ is assigned to the translational degree of freedom perpendicular to the surface.

The fact that there are two different mechanisms active at low incident energies depending on whether the minimal or the maximal coupling is employed becomes evident when inspecting the velocities that the triplet molecules exhibit in the reflection channel. Fig. 6 shows the average kinetic energy gain that an incident singlet molecule experiences when being backscattered as a triplet. Since this data has been derived from the velocities that the reflected triplet molecules exhibit back in vacuum, the plots include both the energy rearrangement due to the nonadiabatic transition, but also all adiabatic energy redistribution processes that occur during the backscattering dynamics. The two different mechanisms active at low incident energies result in a qualitatively different reallocation of the energy. At an incident energy of 0.2 eV for instance, the strongest energy gain occurs in the translational degrees of freedom for the minimal coupling, whereas it occurs in the rotational channel for the maximal coupling.

The fact that the triplet-singlet conversion results in a kinetic energy gain also facilitates the realization of the proposed experiment. At low incident energies, there is no need to detect the electronic character of the backscattered molecules by, e.g., phosphorescence, since energy conservation allows to disentangle the contributions of the two molecular species by measuring the kinetic energy distribution of the reflected molecules[54], even in the case of a mixed triplet/singlet incident molecular beam. If any of the degrees of freedom exhibits an energy that is not compatible with the translational energy that the molecular beam initially exhibits, a transition from the singlet state must have happened. It is thus sufficient to perform a TOF measurement to unambiguously detect a significant amount of triplet oxygen through the respective kinetic energy gain.

D. The frozen substrate approximation

To further substantiate our findings, we also inspected the role of the surface mobility, which has not been accounted for in the hitherto presented calculations. As mentioned before, the employed potential-energy sur-

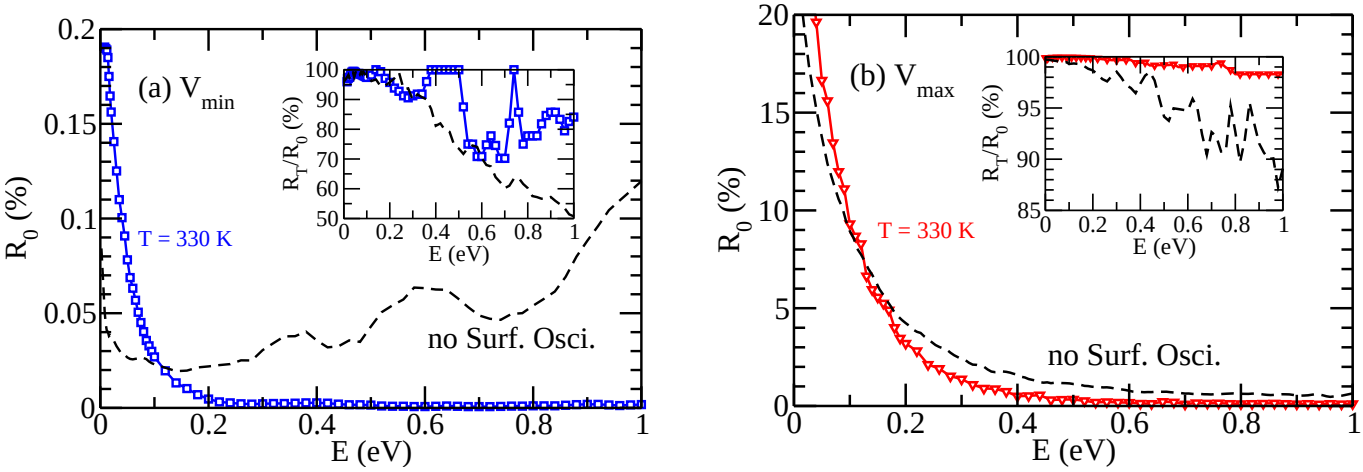

FIG. 7: Reflection coefficient R_0 as function of the incident kinetic energy of singlet oxygen molecules, as calculated by the SH method with a (a) minimal coupling; (b) maximal coupling. The results both within the frozen substrate approximation (dashed lines) and for a three-dimensional surface oscillator (squares and triangles) are shown. In the respective insets, the relative triplet yield R_T/R_0 for both calculations is plotted as well.

faces[14] solely depend upon the degrees of freedom of the oxygen but not on the ones of the aluminum atoms. In this so called *frozen substrate approximation* no energy dissipation into the bulk is possible, so that our description of the dynamics close to the surface, where the adsorption energy of the oxygen molecule is freed, is certainly defective. For the actual triplet dissociation probability at low incident energies, which is basically determined by the barriers present in the entrance channel (see Sec. III A), the dynamics of the bulk atoms can generally be neglected. Still, the frozen substrate approximation might affect the reflection coefficients for the singlet oxygen, in the dynamics of which backscattering processes close to the surface play an important role.

To overcome the frozen substrate approximation we performed simulations with an additional *surface oscillator*[18,46,55], which can account for the possible energy transfer between molecule and bulk in hindsight, i.e., on the basis of potential-energy surfaces derived within the frozen substrate approximation. For this, the aluminum slab is permitted to oscillate as a whole in a harmonic potential, so that the actual molecule-surface distance does then not solely depend on the cartesian center-of-mass coordinate z of the oxygen anymore but also on the amplitude of the surface oscillator $\tilde{z}$. Thus both the diagonal and the non-diagonal potential matrix elements that enter the surface hopping simulations in Eq. (4) and (5) have to be formally adjusted to reflect this additional dependence:

$$V_{ij}\left(\cdots, z, \cdots\right) \xrightarrow{\text{Surf. Osci.}} V_{ij}\left(\cdots, [z-\tilde{z}], \cdots\right). \quad (17)$$

Furthermore, the auxiliary harmonic potential of the slab, which does not depend on the electronic state, is added to each of the diagonal elements of the potential matrix

$$V_{ii}^{7D}(\cdots) = V_{ii}(\cdots) + \frac{\hbar\omega}{2}\tilde{z}^2, \quad (18)$$

whereas no additional coupling term is added to the non-diagonal elements. Analogously, this model can be extended to also allow for an oscillation of the slab with respect to the lateral surface coordinates, as done in all the simulations presented below. Although such a surface oscillator does not yield any additional information about the actual motion of the individual aluminum atoms, it effectively incorporates the energy transfer effects in between the slab and the molecule into the simulations. For the frequency ω of the harmonic potential in Eq. (18) a value of 70% of the experimental Debye frequency (≈ 34 meV) of the bulk[56] has been used, since previous studies showed[57–59] that this fraction is best suited to model the energy dissipation. For the exact same reason three times the mass of a single aluminum atom is assigned to the surface oscillator to account for finite size effects[46,55]. In the herein presented calculations, a kinetic energy that corresponds to a temperature of 330 K has been assigned to the surface vibration in the initial condition. However, no significant dependence on this parameter has been found in the temperature regime at which the experiments are typically performed[3,8,12,60].

Not too surprisingly, the sticking coefficient for incident triplet molecules is hardly affected by the surface oscillator at all due to the fact that this observable is principally determined by the dynamics in the entrance channel. As a matter of fact, absolute changes of $\pm 3\%$ due to the inclusion of the surface oscillator have been found in the simulations at most[50] and are thus not further detailed in this work. In the high energy scattering regime discussed in Sec. III B, however, the already minute reflection coefficients are even further diminished due to the surface mobility.

In contrast to this, the surface oscillator affects the reflection coefficient for singlet molecules in a much more peculiar fashion that sheds light on the underlying transition mechanisms: In the case of a maximal coupling the effects are again minute, as shown in Fig. 7: At large incident velocities, the surface mobility favors dissociation as intuitively expected, since the motion of the aluminum atoms offers a dissipation channel for the incident energy. At low velocities, the inclusion of the surface oscillator leads to a slight increase in the reflectivity. Already when climbing the barriers the molecules lose a small portion of their kinetic energy to the surface oscillator due to Newton's second law. In certain cases, this minute energy transfer is already sufficient to hinder the surmounting of the respective barriers. However, the net effect is again minute, since these processes occur far away from the surface.

We find a more pronounced influence of the surface mobility in the surface hopping calculations with a minimal coupling, as also shown in Fig. 7. At large incident energies the reflection probability drops to zero. The incident molecules become trapped close to the surface due to the energy loss to the surface oscillator when hitting the aluminum, and thus eventually dissociate. The exact same mechanism is active at low incident energies, as also discussed before. However, the energy dissipation through the bulk slows down the oxygen even more, so that a transition to the triplet state becomes more and more probable in spite of the minute coupling value. Accordingly, we find an increase in both the total and the relative yield when the surface atom's mobility is accounted for.

IV. CONCLUSION

In this work we extend previous MD studies[13] of the dissociative adsorption dynamics of oxygen on the aluminum surface by including multiple PESs associated to different spin-configurations in the dynamics by means of Tully's *Fewest Switches* algorithm. Apart from reproducing the experimental sticking coefficient at normal incidence, this approach additionally allows to study the characteristics of the underlying nonadiabatic transitions in detail. This knowledge allows to propose experiments that are able to unambiguously identify the occurrence of such spin-transitions. Whereas the detection of the triplet-to-singlet conversion in high energy scattering experiments is highly unlikely, a non-zero probability for the singlet-to-triplet conversion in scattering experiments with a beam of singlet oxygen molecules has been found, even in the limit of an unrealistically small coupling. If we additionally include the motion of the substrate atoms in our model, the determined yields are either not altered significantly or even enhanced. Depending on the coupling strength, two different mechanisms, which result in different kinetic energy distributions in the reflection channel, have been found in the singlet-to-triplet conversion dynamics. An experimental determination of these distributions does thus allow (a) to prove the nonadiabaticity of this reaction and (b) to draw conclusions on the character of the ongoing transition.

Acknowledgments

Financial grants from the *Deutsche Forschungsgemeinschaft* within the projects RE 1509/7-1 and GR 1503/17-1 is gratefully acknowledged. JB is grateful for financial support by the FCI and the DFG (BE 3264/3-1). Additional computational resources were provided by the D-GRID (bwGRID) project.

[1] N. Cabrera and N. Mott, Rep. Prog. Phys. **12**, 163 (1949).
[2] P. O. Gartland, Surf. Sci. **62**, 183 (1977).
[3] H. Brune, J. Wintterlin, R. J. Behm, and G. Ertl, Phys. Rev. Lett. **68**, 624 (1992).
[4] L. C. Ciacchi and M. C. Payne, Phys. Rev. Lett. **92**, 176104 (2004).
[5] M. L. Neuburger and D. P. Pullman, J. Chem. Phys. **113**, 1249 (2000).
[6] M. Binetti, O. Weiße, E. Hasselbrink, A. J. Komrowski, and A. C. Kummel, Faraday Discuss. **117**, 313 (2000).
[7] A. J. Komrowski, J. Z. Sexton, A. C. Kummel, M. Binetti, O. Weiße, and E. Hasselbrink, Phys. Rev. Lett. **87**, 246103 (2001).
[8] M. Schmid, G. Leonardelli, R. Tscheließnig, A. Biedermann, and P. Varga, Surf. Sci. **478**, L355 (2001).
[9] A. Groß, Surf. Sci. **500**, 347 (2002).
[10] K. Honkala and K. Laasonen, Phys. Rev. Lett. **84**, 705 (2000).
[11] Y. Yourdshahyan, B. Razaznejad, and B. I. Lundqvist, Phys. Rev. B **65**, 075416 (2002).
[12] L. Österlund, I. Zorić, and B. Kasemo, Phys. Rev. B **55**, 15452 (1997).
[13] J. Behler, B. Delley, S. Lorenz, K. Reuter, and M. Scheffler, Phys. Rev. Lett. **94**, 036104 (2005).
[14] J. Behler, B. Delley, K. Reuter, and M. Scheffler, Phys. Rev. B **75**, 115409 (2007).
[15] J. Behler, K. Reuter, and M. Scheffler, Phys. Rev. B **77**, 115421 (2008).
[16] J. C. Tully, J. Chem. Phys. **93**, 1061 (1990).
[17] C. Bach, C. Carbogno, and A. Groß, Israel. J. Chem. **45**, 46 (2005).
[18] C. Carbogno, A. Groß, and M. Rohlfing, Appl. Phys. A **88**, 579 (2007).
[19] C. Carbogno, J. Behler, A. Groß, and K. Reuter, Phys. Rev. Lett. **101**, 096104 (2008).
[20] C. Mosch, C. Koukounas, N. Bacalis, A. Metropoulos,

A. Groß, and A. Mavridis, J. Phys. Chem. C **112**, 6924 (2008).
[21] E. Livshits, R. Baer, and R. Kosloff, J. Phys. Chem. A **113**, 7521 (2009).
[22] J. Behler, S. Lorenz, and K. Reuter, J. Chem. Phys. **127**, 014705 (2007).
[23] J. C. Tully, Faraday Discuss. **110**, 407 (1998).
[24] A. Groß and M. Scheffler, J. Vac. Sci. Technol. A **15**, 1624 (1997).
[25] N. Metropolis, A. W. Rosenbluth, M. N. Rosenbluth, A. H. Teller, and E. Teller, J. Chem. Phys. **21**, 1087 (1953).
[26] M. F. Herman, J. Chem. Phys. **81**, 754 (1984).
[27] D. F. Coker and L. Xiao, J. Chem. Phys. **102**, 496 (1995).
[28] M. Head-Gordon and J. C. Tully, J. Chem. Phys. **103**, 10137 (1995).
[29] G. Katz, R. Kosloff, and Y.Zeiri, J. Chem. Phys. **120**, 3931 (2004).
[30] L. V. Slipchenko and A. I. Krylov, J. Chem. Phys. **117**, 4694 (2002).
[31] O. Gunnarsson and R. O. Jones, J. Chem. Phys. **72**, 5357 (1980).
[32] U. Von Barth, Phys. Rev. A **20**, 1693 (1979).
[33] C. Carbogno et al. (in preparation).
[34] A. J. Cohen, P. Mori-Sánchez, and W. Yang, Science **321**, 792 (2008).
[35] D. R. Kearns, Chem. Rev. **71**, 395 (1971).
[36] C. Schweitzer and R. Schmidt, Chem. Rev. **103**, 1685 (2003).
[37] B. F. Minaev, Int. J. Quant. Chem. **17**, 367 (1980).
[38] R. Klotz and S. D. Peyerimhoff, Mol. Phys. **57**, 573 (1986).
[39] T. l. C. Jansen, S. Rettrup, C. R. Sarma, J. G. Snijders, and P. Palmieri, Int. J. Quant. Chem. **73**, 23 (1999).
[40] H.-J. Werner, P. J. Knowles, R. Lindh, F. R. Manby, M. Schütz, P. Celani, T. Korona, G. Rauhut, R. D. Amos, A. Bernhardsson, et al. (2006), URL `http://www.molpro.net`.
[41] H.-J. Werner and P. J. Knowles, J. Chem. Phys. **89**, 5803 (1988).
[42] B. F. Minaev, O. Vahtras, and H. Ågren, Chem. Phys. **208**, 299 (1996).
[43] H. Schwarz, Int. J. Mass Spec. **237**, 75 (2004).
[44] Q. Wu and T. Van Voorhis, J. Chem. Phys. **125**, 164105 (2006).
[45] C. Bach and A. Groß, Faraday Discuss. **117**, 99 (2000).
[46] C. Bach and A. Groß, J. Chem. Phys. **114**, 6396 (2001).
[47] Y. Yourdshahyan, B. Razaznejad, and B. I. Lundqvist, Solid State Comm. **117**, 531 (2001).
[48] G. Henkelman and H. Jónsson, J. Chem. Phys. **113**, 9978 (2000).
[49] G. Henkelman, B. P. Uberuaga, and H. Jónsson, J. Chem. Phys. **113**, 9901 (2000).
[50] C. Carbogno, Ph.D. Thesis, Ulm University (2009).
[51] A. Groß and M. Scheffler, Chem. Phys. Lett. **256**, 417 (1996).
[52] R. Burgert, H. Schnöckel, A. Grubisic, X. Li, S. T. Stokes, K. H. Bowen, G. Ganteför, B. Kiran, and P. Jena, Science **319**, 438 (2008).
[53] M. Alducin, H. F. Busnengo, and R. Díez Muiño, J. Chem. Phys. **129**, 224702 (2008).
[54] A. A. Krasnovsky Jr. and C. S. Foote, J. Am. Chem. Soc. **115**, 6013 (1993).
[55] C. Bach, T. Klüner, and A. Groß, Chem. Phys. Lett. **376**, 424 (2003).
[56] N. W. Ashcroft and N. D. Mermin, *Solid State Physics* (Saunders College, 1976).
[57] M. Hand and J. Harris, J. Chem. Phys. **92**, 7610 (1990).
[58] A. Groß and W. Brenig, Chem. Phys. **177**, 497 (1993).
[59] A. Groß and W. Brenig, Surf. Sci. **302**, 403 (1994).
[60] O. Weiße, C. Wesenberg, M. Binetti, E. Hasselbrink, C. Corriol, G. R. Darling, and S. Holloway, J. Chem. Phys. **118**, 8010 (2003).
[61] C. A. Mead and D. G. Truhlar, J. Chem. Phys. **77**, 6090 (1982).
[62] We use the adjective "diabatic" for electronic states whose wave function does not depend on the nuclear coordinates[16]. In the quantum chemistry community such an approach is often known as "crude diabatic"[61].
[63] The V5Z correlation consistent basis set and Molpro's default numerical integration parameters have been used for the simulations. The convergence with respect to both the basis set and these parameters have been carefully[33] inspected.
[64] Whereas the oxygen-oxygen and the oxygen-surface distance were optimized during the calculations, the other degrees of freedom, i.e. the rotational ones and the lateral surface coordinates, were kept fixed. A total of 350,000 of such configurations were inspected for each of the histograms shown in Fig. 2b. In each run 20 images were used and the location of the dissociated final state, if there was any in the respective elbow plot, was determined by a crude bisection method. The initial image was kept fixed in the vacuum at 5.0 Å distance from the surface at the equilibrium bond-length of an isolated oxygen molecule.
[65] To construct a single and smooth PES on which the crossing point indeed are the highest barriers, we inspected the adiabatic representation of the triplet-singlet system for a vanishing coupling ($\ll 1$ meV).